Journal of proteome research

pubs.acs.org/jpr

Article

Interaction of Drug Candidates with Various SARS-CoV-2 Receptors: An in Silico Study to Combat COVID-19

Romulo O. Barros,[‡] Fabio L. C. C. Junior,[‡] Wildrimak S. Pereira, Neiva M. N. Oliveira, and Ricardo M. Ramos*

Cite This: *J. Proteome Res.* 2020, 19, 4567−4575

Read Online

ACCESS | Metrics & More | Article Recommendations | Supporting Information

ABSTRACT: The world is currently facing the COVID-19 pandemic caused by the SARS-CoV-2 virus. The pandemic is causing the death of people around the world, and public and social health measures to slow or prevent the spread of COVID-19 are being implemented with the involvement of all members of society. Research institutions are accelerating the discovery of vaccines and therapies for COVID-19. In this work, molecular docking was used to study (in silico) the interaction of 24 ligands, divided into four groups, with four SARS-CoV-2 receptors, Nsp9 replicase, main protease (Mpro), NSP15 endoribonuclease, and spike protein (S-protein) interacting with human ACE2. The results showed that the antimalarial drug Metaquine and anti-HIV antiretroviral Saquinavir interacted with all the studied receptors, indicating that they are potential candidates for multitarget drugs for COVID-19.

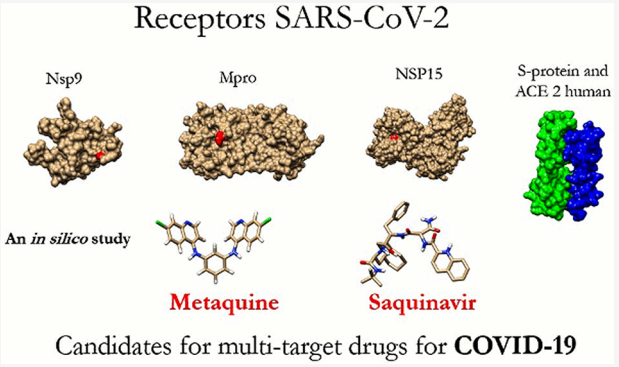

KEYWORDS: *SARS-CoV-2, COVID-19, docking*

INTRODUCTION

The end of 2019 and the beginning of 2020 were marked by the pandemic caused by the severe acute respiratory syndrome coronavirus 2. The first cases of infection by a novel coronavirus (SARS-CoV-2) emerged in December 2019 and were related to exposure to the Huanan Seafood Wholesale Market in the city of Wuhan, Hubei, China.[1,2] The COVID-19 then spread worldwide, and by July 14, 2020, there were 12 964 809 confirmed cases and 570 288 deaths globally.[3] Like SARS-CoV, SARS-CoV-2 seems to use the ACE2 receptor to enter the target cells.[4−8] Alveolar epithelial type II cells are 83% of ACE2-expressing cells,[5] which may explain the higher damage of the infection caused to the lungs, where COVID-19 showed high expression among alveolar epithelial in immunostaining study.[9] There is also evidence that a furin-like cleavage site in the S-protein of SARS-CoV-2 may be implicated in viral invasion of the cells.[10]

In most severe cases of COVID-19, patients require endotracheal intubation and mechanical ventilation, as they may develop severe pneumonia, pulmonary edema, ARDS, sepsis shock, or multiple organ failure.[2−11] The disease affects most severely males more than females, and patients with chronic cardiovascular and cerebrovascular diseases, diabetes, obesity, smoking history, and other comorbidities, resulting in lower immunity, have the worst prognostics.[12−14]

Research institutions are accelerating the discovery of vaccines and therapies for COVID-19. In this work, molecular docking was used to study (in silico) the interaction of 24 ligands with four SARS-CoV-2 receptors. Crystallographic structures of SARS-CoV-2 receptors, Nsp9 replicase protein, main protease (Mpro), and NSP15 endoribonuclease were used. One of the receptors was the model built by homology modeling of the spike protein (S-protein) and the human ACE2 receptor, and obtained in a study by Smith and Smith, 2020.[15] The objective of this work was to study the interactions performed by the ligands on these receptors and to indicate drug candidates for COVID-19.

MATERIALS AND METHODS

3D Structure of Ligands and Receptors

The 3D structures of the ligands were obtained from the PubChem Open Chemistry Database (https://pubchem.ncbi.nlm.nih.gov/) (see Table 2). The ligands were divided into four groups. Group 1 includes six ligands that appear in the recent literature on COVID-19. Group 2 presents the three ligands that obtained the best results in the study by Smith

Special Issue: Proteomics in Pandemic Disease

Received: May 14, 2020
Published: July 27, 2020

https://dx.doi.org/10.1021/acs.jproteome.0c00327
J. Proteome Res. 2020, 19, 4567−4575

Table 1. Information on SARS-CoV-2 Receptors Used

receptor	PDB code/ reference	description	active site region/ interface region
1	6W4B:A	The crystal structure of Nsp9 RNA binding protein of SARS CoV-2. Nsp9 replicase protein. Deposit Date: 2020−03−10.	Lys85
2	6Y84:A	SARS-CoV-2 main protease with unliganded active site (2019-nCoV, coronavirus disease 2019, COVID-19). Deposit Date: 2020−03−03.	Asn142
3	6VWW:A	Crystal structure of NSP15 endoribonuclease from SARS CoV-2. NSP15 endoribonuclease. Deposit Date: 2020−02−20.	His250
4	15	Computational model of the spike protein (S-protein) of SARS-CoV-2 interacting with the human ACE2 receptor. Publication date: 2020−02−27.	15

Table 2. Results of Molecular Docking with Vina

groups	ligand	PubChem CID	receptor 1 ΔG_{bind} (kcal/mol)	receptor 2 ΔG_{bind} (kcal/mol)	receptor 3 ΔG_{bind} (kcal/mol)	receptor 4 ΔG_{bind} (kcal/mol)	references
01	Hydroxychloroquine	3652	−5.0	−5.8	−6.1	−5.4	19−21
	Azithromycin	447043	−4.9	−5.8	−5.6	−6.7	19,22−24
	Mefloquine	40692	−6.8	−7.6	−7.3	−6.7	25
	Metaquine	10670321	−7.5	−8.1	−8.6	−7.9	26,27
	Nelfinavir	64143	−6.1	−7.6	−7.7	−8.0	28,29
	PL-69	25208163	−7.4	−7.2	−7.6	−6.8	30
02	Pemirolast	57697	−5.8	−6.5	−6.0	−7.4	15
	Benserazide	2327	−4.9	−5.9	−5.6	−7.4	15,31
	Luteolin	5280445	−6.1	−7.3	−7.3	−7.4	15,32
03	Saquinavir	441243	−7.3	−7.6	−8.1	−8.6	33,34
	Lopinavir	92727	−6.0	−6.9	−8.0	−7.6	35−37
	Ritonavir	392622	−6.8	−6.8	−7.2	−7.5	35,37
	Piperaquine	122262	−5.7	−7.5	−8.2	−7.4	38
	Dolutegravir	54726191	−6.6	−7.7	−7.8	−8.1	39
04	Fulvic Acid	5359407	−5.4	−7.0	−6.5	−7.0	40,41
	Humic Acid	90472028	−4.6	−5.0	−4.6	−5.9	41
	Piperine	638024	−5.5	−6.4	−6.8	−6.5	42,43
	Rose Oxide	27866	−4.1	−4.2	−4.6	−5.8	44
	Terpineol	17100	−5.3	−4.5	−5.3	−5.8	45
	Ferulate	445858	−4.5	−5.4	−5.6	−5.7	46
	Epicatechin	72276	−5.4	−7.0	−6.8	−6.6	47−49
	Capsaicin	1548943	−5.9	−5.7	−5.9	−5.4	50,51
	Arachidonic Acid	444899	−5.4	−5.0	−5.2	−5.1	49
	Kavain	5281565	−5.1	−5.7	−6.0	−6.2	52

and Smith, 2020.[15] Group 3 is made up of five anti-HIV antiretrovirals, and Group 04 is made up of ten ligands from the database of our research laboratory used in previous studies (Table 2).

Table 1 shows that Receptors 1, 2, and 3 were obtained from the Protein Data Bank (PDB) (https://www.rcsb.org/).[16] Receptor 4 was built by homology modeling and obtained from ref 15.

Molecular Docking

Molecular docking calculations were performed using AutoDock Vina software (https://vina.scripps.edu/).[17] The ligands and proteins were prepared for the calculations with AutoDock Tools (ADT) 1.5.6.[18] Hydrogens were added to both receptors and ligands individually. Gasteiger charges were then calculated by ADT, and nonpolar hydrogens were merged. The size of the grid box was set to 22.5 Å for each axis. The grid boxes were centered on the coordinates of the atoms of residues located in the region of the active site and interface region, as shown in Table 1. The number of modes was set to 50, and the exhaustiveness was set to 24. A total of 96 molecular docking calculations were performed. Binding energy (ΔG_{bind}) values better or equal to −7 kcal/mol were established as a criterion for the efficiency of the interaction.

RESULTS AND DISCUSSION

Table 2 shows the results of the molecular docking calculations and references related to the ligands. The ligands in Groups 1 and 3 were selected for a drug repurposing study for COVID-19, the ligands in Group 2 were selected to analyze the interaction in the receptors of this study, and the ligands in Group 4 are chemical structures of natural compounds.

Regarding the ligands of Group 1, Table 2 shows that hydroxychloroquine and azithromycin did not interact with the receptors, which may indicate that these drugs act in different steps in the viral cycle other than the ones that involve the proteins in this study. The literature cites three probable mechanisms of action for hydroxychloroquine: conformational modification of angiotensin-converting enzyme type 2 (ACE 2), alteration of the pH of the endosome, and reduction and inhibition in the release of pro-inflammatory cytokines (TNF-α and IL-6). Mefloquine showed interaction at Receptors 2 (−7.6 kcal/mol) and 3 (−7.3 kcal/mol). Nelfinavir and PL-69 showed interaction in three of the four studied receptors. Metaquine (*N*,*N*′-Bis(7-chloro-4-quinolyl)-*m*-phenylenediamine), mentioned in the literature as an antimalarial substance,[26] presented relevant

https://dx.doi.org/10.1021/acs.jproteome.0c00327
J. Proteome Res. 2020, 19, 4567−4575

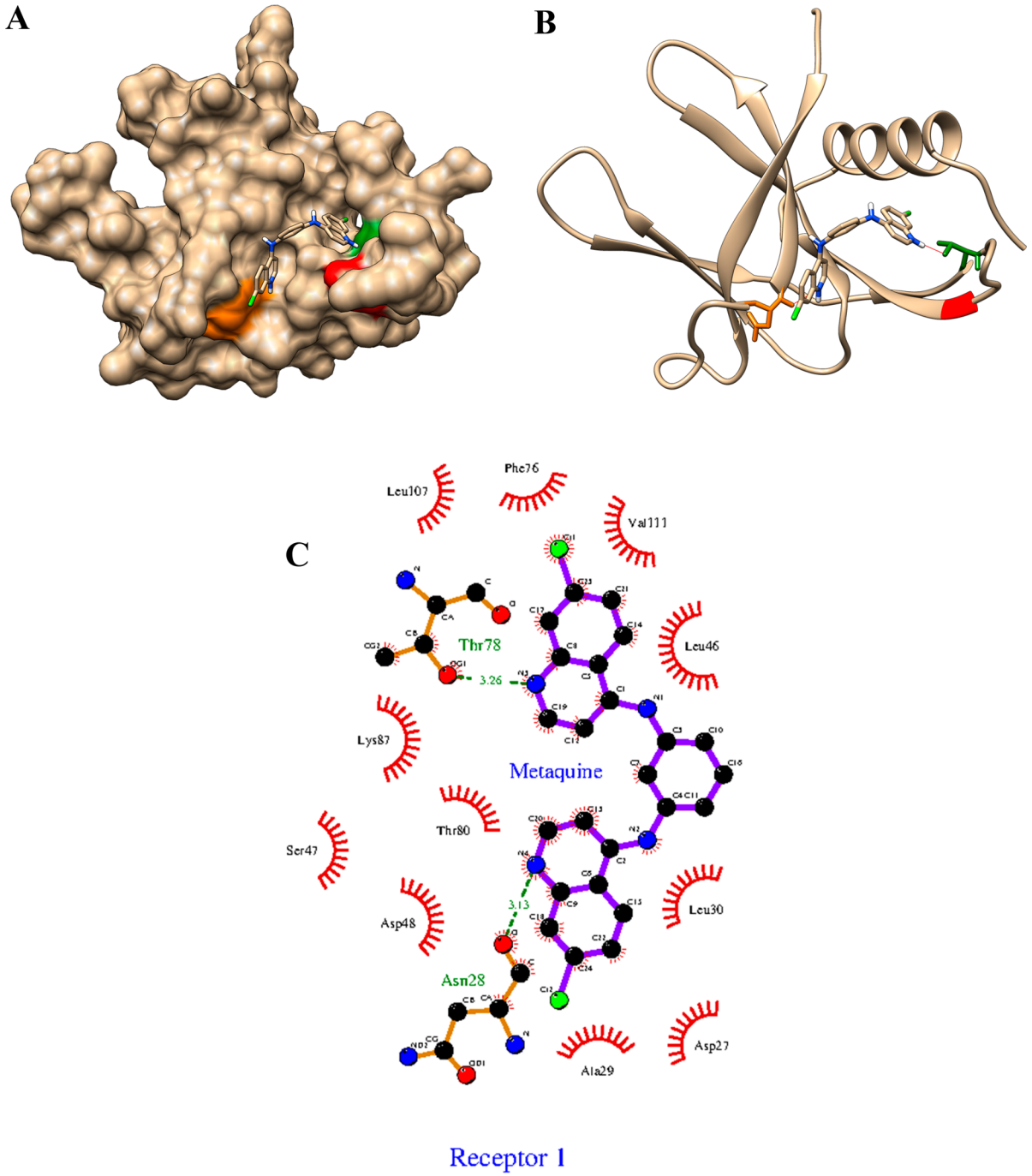

Figure 1. Global structure of the conformations resulted from docking. (A) Surface representation. (B) Representation in ribbons. Asn28 orange, Thr78 green, Lys85 red, Metaquine CPK, in sticks. (C) LigPlot+ diagram of the Receptor 1_Metaquine interaction [ref 53]. Figure was generated using UCSF Chimera (https://www.cgl.ucsf.edu/chimera/) [ref 54].

results of interaction in all receptors, mainly in Receptor 3, where the binding energy was equal to −8.6 kcal/mol (see Figure 3).

The ligands in Group 02 showed relevant results in receptor 4 according to the study the of Smith and Smith, 2020.[15] In this study, Pemirolast and Benserazide ligands did not show any relevant interaction with the other three receptors. Luteolin showed an interaction with a binding energy value of −7.3 kcal/mol with Receptors 2 and 3. The results obtained for the three ligands at Receptor 4 (−7.4 kcal/mol) are in accordance with the study of Smith and Smith, 2020.[15]

Among Group 3 ligands, Lopinavir and Ritonavir showed interaction at two of the four receptors, Piperaquine and Dolutegravir had better results and showed interactions with three receptors. Saquinavir showed interaction with all receptors, with highlights to binding energy value of −8.6 kcal/mol at Receptor 4 (see Figure 4).

Regarding the ligands in Group 4, these did not present relevant results. What stood out the most in this group was Fulvic Acid, with a result of binding energy equal to −7 kcal/mol with Receptors 2 and 4. Epicatechin showed the same result with Receptor 2.

https://dx.doi.org/10.1021/acs.jproteome.0c00327
J. Proteome Res. 2020, 19, 4567−4575

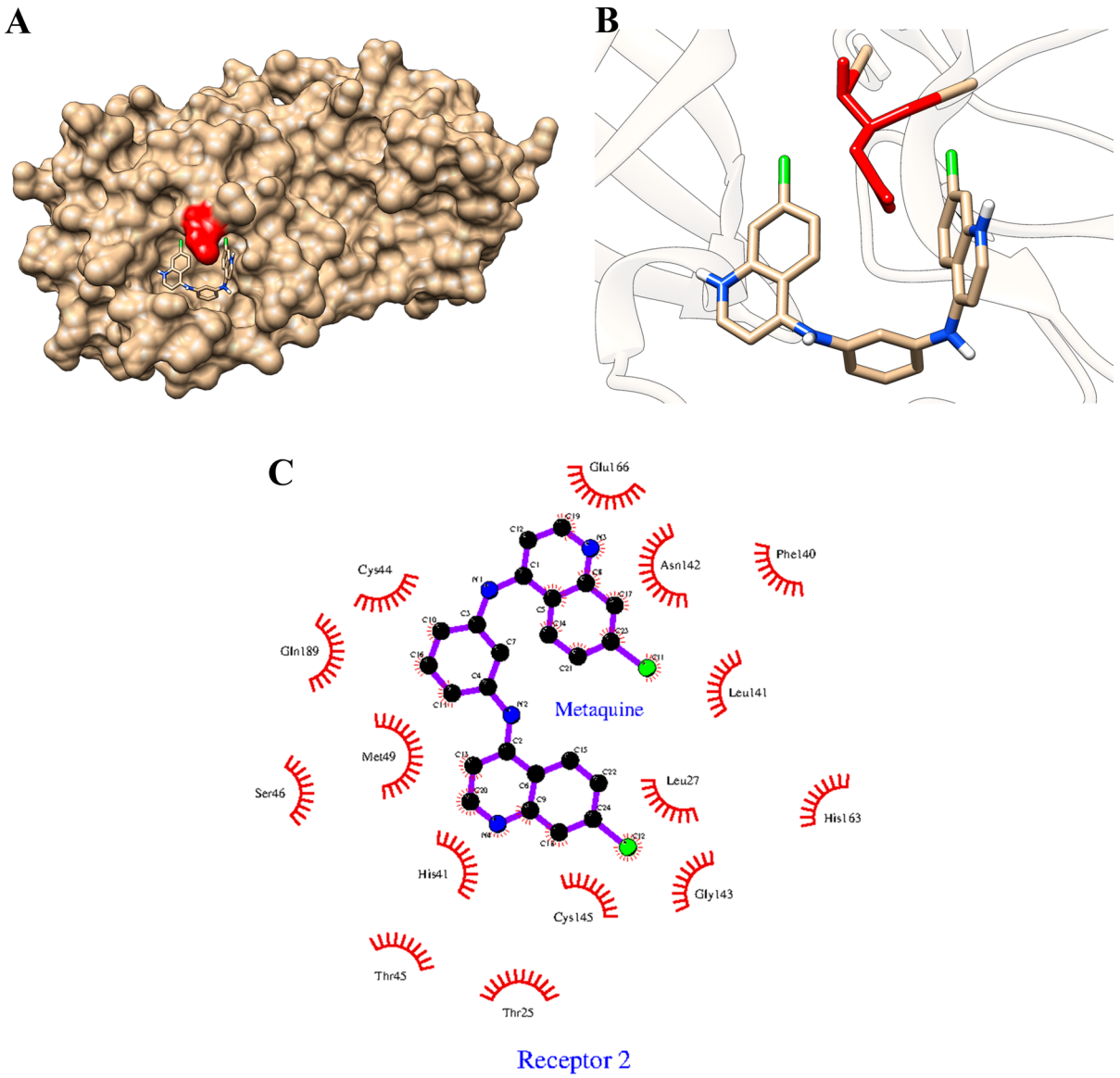

Figure 2. Global structure of the conformations resulted from docking. (A) Surface representation. (B) Representation of the region of the active site enlarged in transparent ribbons. Asn142 red, Metaquine CPK, by sticks. (C) LigPlot+ diagram of the Receptor 2_Metaquine interaction.

The results show that Saquinavir (Group 1) and Metaquine (Group 3) showed interaction with all the receptors in this study, indicating that these two drugs can be repurposed for the treatment of COVID-19. Nelfinavir and PL-69 (Group 1), Luteolin (Group 2), and Piperaquine and Dolutegravir (Group 3) interacted with three receptors and cannot be excluded as multitarget drug candidates for COVID-19. In silico studies can be carried out by changing the geometry of these ligands in order to improve the binding energy in the studied receptors; besides, in vitro and in vivo studies must be carried out to make promising drug candidates.

Metaquine is a potent, soluble, and bioavailable antimalarial substance. Metaquin shows activity in vivo (oral ID50 of 25 μmol/kg) against *Plasmodium berghei* and in vitro (0.17 μM) against *Plasmodium falciparum* K1 multidrug-resistant. Metaquin shows strong affinity for the putative heme antimalarial receptor.[26] Fielding et al.[27] showed that the inclusion of trifluoromethyl (CF3) in the chemical structure of Metaquine had a great impact on the drug interaction with the heme antimalarial receptor.

Saquinavir is a specific inhibitor drug for HIV protease. Jayaswal et al.[34] carried out an in silico study with modified Saquinavir structures to test the interaction with the HIV protease active site, with the aim of finding structures that present better binding energy than Saquinavir. Khadim et al.[33] conducted an in silico study of the interaction of SARS-Cov-2 main protease (Mpro) with anti-HIV drugs. The results obtained are in agreement with our study indicating that Saquinavir presented interactions with Mpro.

Figures 1−4 show information about the complexes with the best binding energy for each receptor. Regarding the LigPlot+ diagrams, Figures 1C, 2C, 3C, and 4C, the hydrogen bonds are represented by green dotted lines and the hydrophobic contacts are represented by red semicircles. The value that appears on the hydrogen bonds corresponds to the distance, in angstroms, between the amino acid residue of the protein and the ligand. Figures S1, S2, and S3 show interaction of Saquinavir at Receptors 1, 2, and 3, respectively, and Figure S4 shows the interaction of Metaquine at Receptor 4.

https://dx.doi.org/10.1021/acs.jproteome.0c00327
J. Proteome Res. 2020, 19, 4567−4575

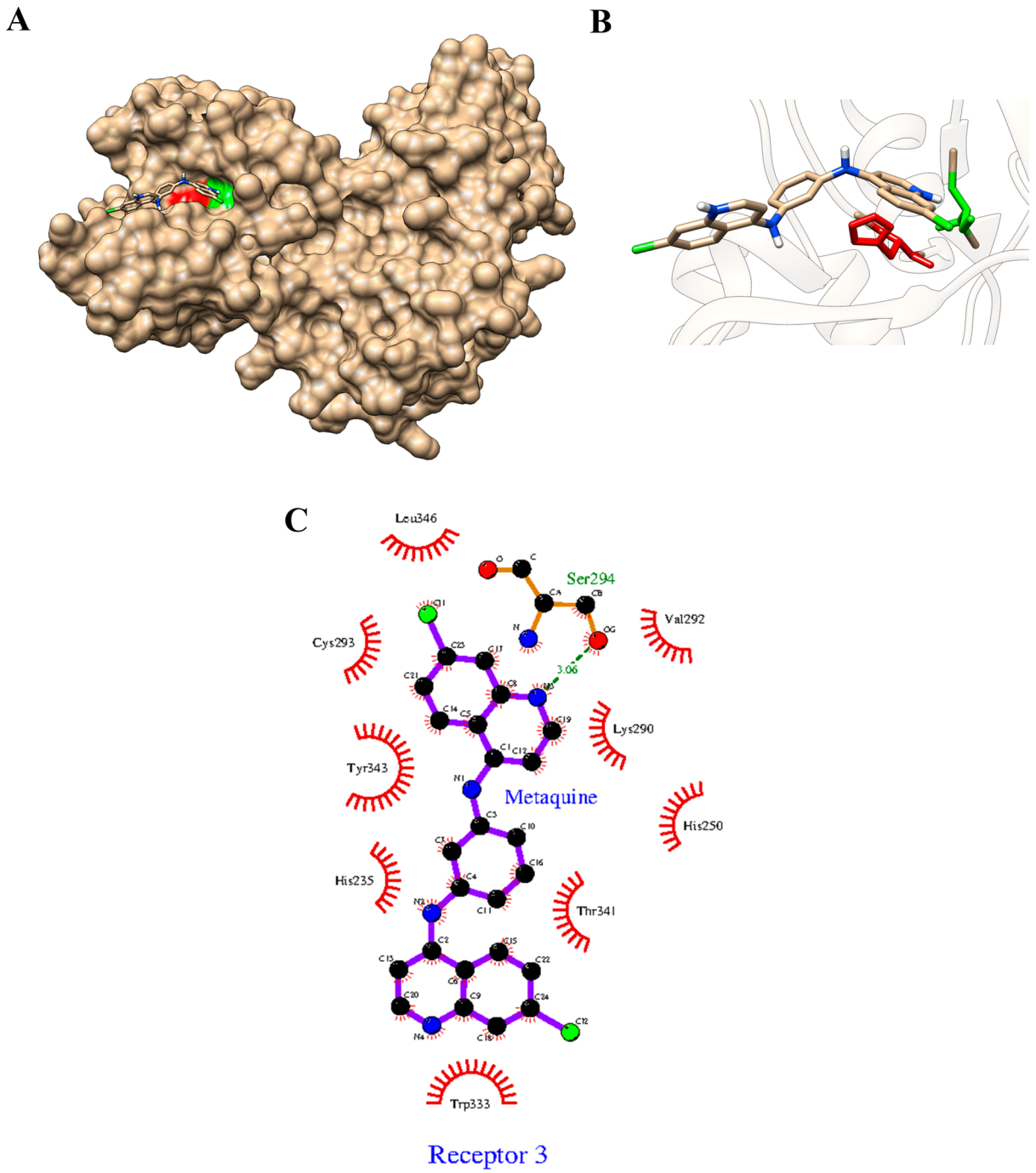

Figure 3. Global structure of the conformations resulted from docking. (A) Surface representation. (B) Representation of the region of the active site enlarged in transparent ribbons. His250 red, Ser294 green, Metaquine CPK, by sticks. (C) LigPlot+ diagram of the Receptor 3_Metaquine interaction.

Figure 1C shows that Metaquine performed two interactions by hydrogen bonds with Receptor 1 (residues Asn28 and Thr78) and 11 interactions by hydrophobic contacts (residues Phe76, Val111, Leu46, Leu30, Asp27, Ala29, Asp48, Thr80, Ser47, Lys87, and Leu107).

Figure 2A shows the conformation of Metaquine in a cavity of Receptor 2 near the Asn142 residue (in red) in the region of the active site (see Table 1). In Figure 2C, it is shown that Metaquine interacted by hydrophobic contacts with 15 residues (Asn142—active site, Glu166, Phe140, Leu141, Leu27, His163, Gly143, Cys145, Thr25, Thr45, His41, Met49, Ser46, Gln189, and Cys44).

Figure 3A shows the conformation of the Metaquine in a cavity of Receptor 3 near His250 (in red) in the region of the active site.

In Receptor 3, Metaquine performed an interaction by hydrogen bond (Ser294) and nine interactions by hydrophobic contacts (Val292, Lys290, His250—active site, Thr341, Trp333, His235, Tyr343, Cys293, and Leu346). Figure 4 shows a part of the model created for human ACE2 receptor in green and part of the model created for spike protein (S-protein) in blue.

These parts of the two models were selected for molecular docking studies (see ref 15). As it can be seen in Figure 4A,

https://dx.doi.org/10.1021/acs.jproteome.0c00327
J. Proteome Res. 2020, 19, 4567−4575

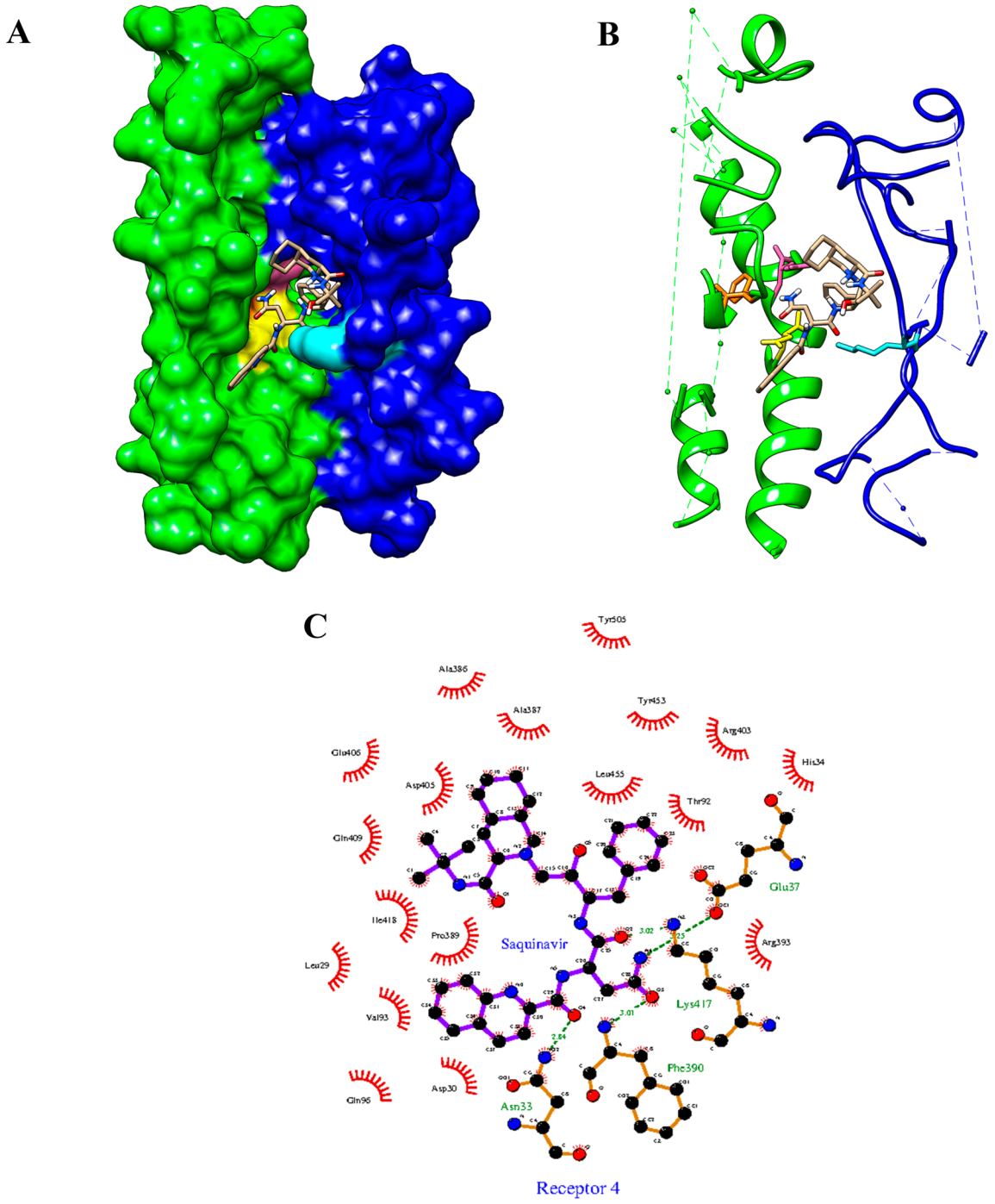

Figure 4. Global structure of the conformations results from docking. (A) Surface representation. (B) Representation in ribbons. Asn33 yellow, Glu37 pink, Phe390 orange, Lys417 cyan, Saquinavir CPK, by sticks. (C) LigPlot+ diagram of the Receptor 4_Saquinavir interaction.

Saquinavir is positioned in the expected region, between the ACE2 receptor and the S-protein. Figure 4C shows that Saquinavir performed four interactions by hydrogen bond, three of them with the ACE2 receptor (Asn33, Glu37, and Phe390) and one with the S-protein (Lys417). In addition, it performed 18 interactions by hydrophobic contact with both models.

CONCLUSIONS

The results confirmed the interaction of Metaquine (*N*,*N*′-Bis(7-chloro-4-quinolyl)-*m*-phenylenediamine) and Saquinavir in all receptors studied, indicating them as candidates for multitarget drugs that can be repurposed to the treatment of COVID-19. In vitro, in vivo, and clinical tests should be performed to confirm the effectiveness of these drugs in the treatment of COVID-19.

ASSOCIATED CONTENT

Supporting Information

The Supporting Information is available free of charge at https://pubs.acs.org/doi/10.1021/acs.jproteome.0c00327.

Figures S1−S4: Global structure of the conformations resulted from docking (PDF)

https://dx.doi.org/10.1021/acs.jproteome.0c00327
J. Proteome Res. 2020, 19, 4567−4575

AUTHOR INFORMATION

Corresponding Author

Ricardo M. Ramos − *Research Laboratory in Information Systems, Department of Information, Environment, Health and Food Production, Federal Institute of Piaui, LaPeSI/IFPI, Teresina, Piaui 64019-368, Brazil;* orcid.org/0000-0003-2016-3344; Phone: +55 86 99442-1780; Email: ricardo@ifpi.edu.br

Authors

Romulo O. Barros − *Research Laboratory in Information Systems, Department of Information, Environment, Health and Food Production, Federal Institute of Piaui, LaPeSI/IFPI, Teresina, Piaui 64019-368, Brazil*

Fabio L. C. C. Junior − *Research Laboratory in Information Systems, Department of Information, Environment, Health and Food Production, Federal Institute of Piaui, LaPeSI/IFPI, Teresina, Piaui 64019-368, Brazil*

Wildrimak S. Pereira − *Research Laboratory in Information Systems, Department of Information, Environment, Health and Food Production, Federal Institute of Piaui, LaPeSI/IFPI, Teresina, Piaui 64019-368, Brazil*

Neiva M. N. Oliveira − *Research Laboratory in Information Systems, Department of Information, Environment, Health and Food Production, Federal Institute of Piaui, LaPeSI/IFPI, Teresina, Piaui 64019-368, Brazil*

Complete contact information is available at: https://pubs.acs.org/10.1021/acs.jproteome.0c00327

Author Contributions

‡R.O.B. and F.L.C.C.J. contributed equally to this work.

Notes

The authors declare no competing financial interest.

ACKNOWLEDGMENTS

We thank the professors of the Graduate Program in Chemistry (PPGQ), especially Prof. Dr. Antônio Luiz Martins Maia Filho, Prof. Dr. Francielle Alline Martins, and Prof. Dr. Valdiléia Teixeira Uchoa from the State University of Piauí. Prof. Dr. Francisco das Chagas Alves Lima and Prof. Dr. Rosemarie Brandim Marques, from the State University of Piauí. To the professors of the Department of Information, Environment, Health and Food Production (DIASPA), especially Prof. Dr. Bruna de Freitas Iwata and Prof. Dr. Rosana Martins Carneiro, from the Federal Institute of Piauí. We thank the Federal Institute of Piauí for financial support.

REFERENCES

(1) Li, Q.; Guan, X.; Wu, P.; Wang, X.; Zhou, L.; Tong, Y.; et al. Early Transmission Dynamics in Wuhan, China, of Novel Coronavirus−Infected Pneumonia. *N. Engl. J. Med.* **2020**, *382*, 1199−1207.

(2) Chen, N.; Zhou, M.; Dong, X.; Qu, J.; Gong, F.; Han, Y.; et al. Epidemiological and clinical characteristics of 99 cases of 2019 novel coronavirus pneumonia in Wuhan, China: a descriptive study. *Lancet* **2020**, *395*, 507−513.

(3) World Health Organization. *Coronavirus Disease 2019 (COVID-19). Situation Report. 2020 July Report No.: 176.*

(4) Zhang, H.; Penninger, J. M.; Li, Y.; Zhong, N.; Slutsky, A. S. Angiotensin-converting enzyme 2 (ACE2) as a SARS-CoV-2 receptor: molecular mechanisms and potential therapeutic target. *Intensive Care Med.* **2020**, *46*, 586−590.

(5) Zhao, Y.; Zhao, Z.; Wang, Y.; Zhou, Y.; Ma, Y.; Zuo, W. Single-cell RNA expression profiling of ACE2, the putative receptor of Wuhan 2019-nCov. *bioRxiv*, Jan 26, 2020, DOI: 10.1101/2020.01.26.919985 (accessed 2020-04-16).

(6) Zhou, P.; Yang, X.-L.; Wang, X.-G.; Hu, B.; Zhang, L.; Zhang, W.; et al. A pneumonia outbreak associated with a new coronavirus of probable bat origin. *Nature* **2020**, *579*, 270−273.

(7) Xu, X.; Chen, P.; Wang, J.; Feng, J.; Zhou, H.; Li, X.; et al. Evolution of the novel coronavirus from the ongoing Wuhan outbreak and modeling of its spike protein for risk of human transmission. *Sci. China: Life Sci.* **2020**, *63*, 457−460.

(8) Hoffmann, M.; Kleine-Weber, H.; Schroeder, S.; Krüger, N.; Herrler, T.; Erichsen, S.; et al. SARS-CoV-2 Cell Entry Depends on ACE2 and TMPRSS2 and Is Blocked by a Clinically Proven Protease Inhibitor. *Cell* **2020**, *181*, 271−280.e8.

(9) Zhang, H.; Zhou, P.; Wei, Y.; Yue, H.; Wang, Y.; Hu, M.; et al. Histopathologic Changes and SARS−CoV-2 Immunostaining in the Lung of a Patient With COVID-19. *Ann. Intern. Med.* **2020**, *172*, 629.

(10) Coutard, B.; Valle, C.; de Lamballerie, X.; Canard, B.; Seidah, N. G.; Decroly, E. The spike glycoprotein of the new coronavirus 2019-nCoV contains a furin-like cleavage site absent in CoV of the same clade. *Antiviral Res.* **2020**, *176*, 104742.

(11) Jiang, F.; Deng, L.; Zhang, L.; Cai, Y.; Cheung, C. W.; Xia, Z. Review of the Clinical Characteristics of Coronavirus Disease 2019 (COVID-19). *Journal of General Internal Medicine* **2020**, *35*, 1545.

(12) Wang, L.; Wang, Y.; Ye, D.; Liu, Q. A review of the 2019 Novel Coronavirus (COVID-19) based on current evidence. *Int. J. Antimicrob. Agents* **2020**, *55*, 105948.

(13) Chavez, S.; Long, B.; Koyfman, A.; Liang, S. Y. Coronavirus Disease (COVID-19): A primer for emergency physicians. *Am. J. Emerg. Med.* **2020**, DOI: 10.1016/j.ajem.2020.03.036.

(14) Yang, J.; Zheng, Y.; Gou, X.; Pu, K.; Chen, Z.; Guo, Q.; et al. Prevalence of comorbidities in the novel Wuhan coronavirus (COVID-19) infection: a systematic review and meta-analysis. *Int. J. Infect. Dis.* **2020**, *94*, 91.

(15) Smith, M.; Smith, J. C. Repurposing Therapeutics for COVID-19: Supercomputer-Based Docking to the SARS-CoV-2 Viral Spike Protein and Viral Spike Protein-Human ACE2 Interface. *ChemRxiv*, Feb 20, 2020, DOI: 10.26434/chemrxiv.11871402.v3 (accessed 2020-04-01).

(16) Berman, H. M.; Westbrook, J.; Feng, Z.; Gilliland, G.; Bhat, T. N.; Weissig, H.; Shindyalov, I. N.; Bourne, P. E. The Protein Data. *Bank Nucleic Acids Research* **2000**, *28*, 235−242.

(17) Trott, O.; Olson, A. J. AutoDock Vina: improving the speed and accuracy of docking with a new scoring function, efficient optimization, and multithreading. *J. Comput. Chem.* **2009**, *31*, 455−461.

(18) Morris, G. M.; Huey, R.; Lindstrom, W.; Sanner, M. F.; Belew, R. K.; Goodsell, D. S.; Olson, A. J.; et al. AutoDock4 and AutoDockTools4: Automated Docking with Selective Receptor Flexibility. *J. Comput. Chem.* **2009**, *30*, 2785−2791.

(19) Gautret, P.; Lagier, J. C.; Parola, P.; Hoang, V. T.; Meddeb, L.; Mailhe, M.; Dourdier, B.; et al. Hydroxychloroquine and azithromycin as a treatment of COVID-19: results of an open-label non-randomized clinical trial. *Int. J. Antimicrob. Agents* **2020**, *56*, 105949.

(20) Sahraei, Z.; Shabani, M.; Shokouhi, S.; Saffaei, A. Aminoquinolines against coronavirus disease 2019(COVID-19): chloroquine or hydroxychloroquine. *Int. J. Antimicrob. Agents* **2020**, *55*, 105945.

(21) Singh, A. K.; Singh, A.; Shaikh, A.; Singh, R.; Misra, A. Chloroquine and hydroxychloroquine in the treatment of COVID-19 with or without diabetes: A systematic search and a narrative review with a special reference to India and other developing countries. *Diabetes Metab. Syndr.: Clin. Res. Rev.* **2020**, *14*, 241−246.

(22) Weng, D.; Wu, Q.; Chen, X.-Q.; Du, Y.-K.; Chen, T.; Li, H.; Tang, D.-L.; Li, Q.-H.; Zhang, Y.; Lu, L.-Q.; Zhou, N.-Y.; Song, J.-C.; Wang, C.; Li, H.-P. Azithromycin treats diffuse panbronchiolitis by

targeting T cells via inhibition of mTOR pathway. *Biomed. Pharmacother.* **2019**, *110*, 440−448.
(23) Kawamura, K.; Ichikado, K.; Takaki, M.; Eguchi, Y.; Anan, K.; Suga, M. Adjunctive therapy with azithromycin for moderate and severe acute respiratory distress syndrome: a retrospective, propensity score-matching analysis of prospectively collected data at a single center. *Int. J. Antimicrob. Agents* **2018**, *51*, 918−924.
(24) Zeng, S.; Meng, X.; Huang, Q.; Lei, N.; Zeng, L.; Jiang, X.; Guo, X. Spiramycin and azithromycin, safe for administration to children, exert antiviral activity against enterovirus A71 in vitro and in vivo. *Int. J. Antimicrob. Agents* **2019**, *53*, 362−369.
(25) Liu, Y.; Chan, W.; Wang, Z.; Hur, J.; Xie, J.; Yu, H.; He, Y. Ontological and bioinformatic analysis of anti-coronavirus drugs and their implication for drug repurposing against COVID-19. *Preprints*, Mar 29, 2020, DOI: 10.20944/preprints202003.0413.v1 (accessed 2020-04-01).
(26) Dascombe, M. J.; Drew, M. G.; Morris, H.; Wilairat, P.; Auparakkitanon, S.; Moule, W. A.; Alizadeh-Shekalgourabi, S.; Evans, P. G.; Lloyd, M.; Dyas, A. M.; Carr, P.; Ismail, F. M. D. Mapping Antimalarial Pharmacophores as a Useful Tool for the Rapid Discovery of Drugs Effective in Vivo: Design, Construction, Characterization, and Pharmacology of Metaquine. *J. Med. Chem.* **2005**, *48* (17), 5423−5436.
(27) Fielding, A. J.; Lukinovic, V.; Evans, P. G.; Alizadeh-Shekalgourabi, S.; Bisby, R. H.; Drew, M. G. B.; Male, V.; Del Casino, A.; Dunn, J. F.; Randle, L. E.; Dempster, N. M.; Nahar, L.; Sarker, S. D.; Cantu Reinhard, F. G.; de Visser, S. P.; Dascombe, M. J.; Ismail, F. M. D. Modulation of Antimalarial Activity at a Putative Bisquinoline Receptor In Vivo Using Fluorinated Bisquinolines. *Chem. A Eur. J.* **2017**, *23* (28), 6811−6828.
(28) Sekhar, T. Virtual Screening based prediction of potential drugs for COVID-19. *Preprints*, Feb 28, 2020, DOI: 10.20944/preprints202002.0418.v2 (accessed 2020-04-01).
(29) Xu, Z.; Peng, C.; Shi, Y.; Zhu, Z.; Mu, K.; Wang, X. Nelfinavir was predicted to be a potential inhibitor of 2019-nCov main protease by an integrative approach combining homology modelling, molecular docking and binding free energy calculation. *bioRxiv*, Jan 28, 2020, DOI: 10.1101/2020.01.27.921627 (accessed 2020-04-01).
(30) Burgess, S. J.; Kelly, J. X.; Shomloo, S.; Wittlin, S.; Brun, R.; Liebmann, K.; Peyton, D. H. Peyton DH. Synthesis, structure-activity relationship, and mode-of-action studies of antimalarial reversed chloroquine compounds. *J. Med. Chem.* **2010**, *53*, 6477.
(31) Shabani-Nooshabadi, M.; Roostaee, M.; Karimi-Maleh, H. Incorporation of graphene oxide−NiO nanocomposite and n-hexyl-3-methylimidazolium hexafluoro phosphate into carbon paste electrode: application as an electrochemical sensor for simultaneous determination of benserazide, levodopa and tryptophan. *J. Iran. Chem. Soc.* **2017**, *14*, 955−961.
(32) Wang, H.; Luo, Y.; Qiao, T.; et al. Luteolin sensitizes the antitumor effect of cisplatin in drug-resistant ovarian cancer via induction of apoptosis and inhibition of cell migration and invasion. *J. Ovarian Res.* **2018**, *11*, 11.
(33) Khadim, S.; Hamdullah, A.; Tanzila, M.; Zainab, S.; Arshad, I.; Hassan, M. pH Dependent Differential Binding Behavior of Prtotease Inhibitor Molecular Drugs for SARS-COV-2. *ChemRxiv*, Mar 20, 2020, DOI: 10.26434/chemrxiv.12009018.v1 (accessed 2020-04-01).
(34) Jayaswal, A.; Mishra, H.; Mishra, A.; Shah, K. Examining pharmacodynamic and pharmacokinetic properties of eleven analogues of saquinavir for HIV protease inhibition. *Arch. Virol.* **2019**, *164*, 949−960.
(35) Kang, S.; Peng, W.; Zhu, Y.; Lu, S.; Zhou, M.; Lin, W.; Wu, W.; Huang, S.; Jiang, L.; Luo, X.; Deng, M. Recent Progress in understanding 2019 Novel Coronavirus associated with Human Respiratory Disease: Detection, Mechanism and Treatment. *Int. J. Antimicrob. Agents* **2020**, *55*, 105950.
(36) Liu, F.; Xu, A.; Zhang, Y.; Xuan, W.; Yan, T.; Pan, K.; Yu, W.; Zhang, J. Patients of COVID-19 may benefit from sustained lopinavir-combined regimen and the increase of eosinophil may predict the outcome of COVID-19 progression. *Int. J. Infect. Dis.* **2020**, *95*, 183.
(37) Lim, J.; Jeon, S.; Shin, H. Y.; Kim, M. J.; Seong, Y. M.; Lee, W. J.; Choe, K. W.; Kang, Y. M.; Lee, B.; Park, S. J. Case of the Index Patient Who Caused Tertiary Transmission of Coronavirus Disease 2019 in Korea: the Application of Lopinavir/Ritonavir for the Treatment of COVID-19 Pneumonia Monitored by Quantitative RT-PCR. *J. Korean Med. Sci.* **2020**, *35*, e79.
(38) Desai, M.; Gutman, J.; L'lanziva, A.; Otieno, K.; Juma, E.; Kariuki, S.; et al. Intermittent screening and treatment or intermittent preventive treatment with dihydroartemisinin−piperaquine versus intermittent preventive treatment with sulfadoxine−pyrimethamine for the control of malaria during pregnancy in western Kenya: an open-label, three-group, randomised controlled superiority trial. *Lancet* **2015**, *386*, 2507−2519.
(39) Walmsley, S. L.; Antela, A.; Clumeck, N.; Duiculescu, D.; Eberhard, A.; Gutierrez, F.; Hocqueloux, L.; Maggiolo, F.; Sandkovsky, U.; Granier, C.; Pappa, K.; Wynne, B.; Min, S.; Nichols, G. Dolutegravir plus Abacavir−Lamivudine for the Treatment of HIV-1 Infection. *N. Engl. J. Med.* **2013**, *369*, 1807−1818.
(40) Zhao, Y.; Paderu, P.; Delmas, G.; Dolgov, E.; Lee, M. H.; Senter, M.; et al. Carbohydrate-derived fulvic acid is a highly promising topical agent to enhance healing of wounds infected with drug-resistant pathogens. *J. Trauma Acute Care Surg.* **2015**, *79*, S121−S129.
(41) Wang, Y.; Li, Y.; Zhang, Y.; Wei, W. Effects of macromolecular humic/fulvic acid on Cd (II) adsorption onto reed-derived biochar as compared with tannic acid. *Int. J. Biol. Macromol.* **2019**, *134*, 43−55.
(42) Ezawa, T.; Inoue, Y.; Murata, I.; Takao, K.; Sugita, Y.; Kanamoto, I. Characterization of the dissolution behavior of piperine/cyclodextrins inclusion complexes. *AAPS PharmSciTech* **2018**, *19*, 923−933.
(43) Manayi, A.; Nabavi, S. M.; Setzer, W. N.; Jafari, S. Piperine as a potential anti-cancer agent: a review on preclinical studies. *Curr. Med. Chem.* **2019**, *25*, 4918.
(44) Narnoliya, L. K.; Kaushal, G.; Singh, S. P.; Sangwan, R. S. De novo transcriptome analysis of rose-scented geranium provides insights into the metabolic specificity of terpene and tartaric acid biosynthesis. *BMC Genomics* **2017**, *18*, 74.
(45) Chen, Y.; Weng, Y.; Zhou, M.; Meng, Y.; Liu, J.; Yang, L.; Zuo, Z. Linalool-and α-terpineol-induced programmed cell death in Chlamydomonas reinhardtii. *Ecotoxicol. Environ. Saf.* **2019**, *167*, 435−440.
(46) Hashizume, K.; Ito, T.; Shirato, K.; Amano, N.; Tokiwano, T.; Ohno, T.; Shindo, S.; Watanabe, S.; Okuda, M. Factors affecting levels of ferulic acid, ethyl ferulate and taste-active pyroglutamyl peptides in sake. *J. Biosci. Bioeng.* **2020**, *129*, 322−326.
(47) Xing, J.; Yu, Z.; Zhang, X.; Li, W.; Gao, D.; Wang, J.; Ma, X.; Nie, X.; Wang, W. Epicatechin alleviates inflammation in lipopolysaccharide-induced acute lung injury in mice by inhibiting the p38 MAPK signaling pathway. *Int. Immunopharmacol.* **2019**, *66*, 146−153.
(48) Shariati, S.; Kalantar, H.; Pashmforoosh, M.; Mansouri, E.; Khodayar, M. J. Epicatechin protective effects on bleomycin-induced pulmonary oxidative stress and fibrosis in mice. *Biomed. Pharmacother.* **2019**, *114*, 108776.
(49) Sousa Carvalho, G. F.; Marques, L. K.; Sousa, H. G.; Silva, L. R.; Leão Ferreira, D. C.; Pires de Moura do Amaral, F.; et al. Phytochemical study, molecular docking, genotoxicity and therapeutic efficacy of the aqueous extract of the stem bark of Ximenia americana L. in the treatment of experimental COPD in rats. *J. Ethnopharmacol.* **2020**, *247*, 112259.
(50) Balleza-Tapia, H.; Dolz-Gaiton, P.; Andrade-Talavera, Y.; Fisahn, A. Capsaicin-Induced Impairment of Functional Network Dynamics in Mouse Hippocampus via a TrpV1 Receptor-Independent Pathway: Putative Involvement of Na+/K+-ATPase. *Mol. Neurobiol.* **2020**, *57*, 1170−1185.
(51) Rosenberger, D. C.; Binzen, U.; Treede, R. D.; Greffrath, W. The capsaicin receptor TRPV1 is the first line defense protecting

from acute non damaging heat: a translational approach. *J. Transl. Med.* **2020**, *18*, 1−16.
(52) Ferreira, J. V.; Braga, A. V.; de Resende Machado, R.; Michel, D.; Pianetti, G. A.; El-Aneed, A.; César, I. C. Liquid chromatography-tandem mass spectrometry bioanalytical method for the determination of kavain in mice plasma: Application to a pharmacokinetic study. *J. Chromatogr. B: Anal. Technol. Biomed. Life Sci.* **2020**, *1137*, 121939.
(53) Laskowski, R. A.; Swindells, M. B. LigPlot+: multiple ligand−protein interaction diagrams for drug discovery. *J. Chem. Inf. Model.* **2011**, *51*, 2778−2786.
(54) Pettersen, E. F.; Goddard, T. D.; Huang, C. C.; Couch, G. S.; Greenblatt, D. M.; Meng, E. C.; Ferrin, T. E. UCSF Chimera—a visualization system for exploratory research and analysis. *J. Comput. Chem.* **2004**, *25*, 1605−1612.

https://dx.doi.org/10.1021/acs.jproteome.0c00327
J. Proteome Res. 2020, 19, 4567−4575